A New Functional Model Complex of Extradiol-cleaving Catechol Dioxygenases: Properties and Reactivity of $[Fe^{II}(BLPA)DBCH]BPh_4$

Ji H. Lim, Tae H. Park, Ho-Jin Lee, Kang-Bong Lee,† and Ho G. Jang*

Department of Chemistry, Korea University, Seoul 136-701, Korea
†Advanced Analysis Center, KIST, Seoul 136-130, Korea
Received September 1, 1999

$[Fe^{II}(BLPA)DBCH]BPh_4$ (**1**), a new functional model for the extradiol-cleaving catechol dioxygenases, has been synthesized, where BLPA is bis(6-methyl-2-pyridylmethyl)(2-pyridylmethyl)amine and DBCH is 3,5-di-*tert*-butylcatecholate monoanion. ^1H NMR and EPR studies confirm that **1** has a high-spin Fe(II) (S = 2) center. The electronic spectrum of **1** exhibits one absorption band at 386 nm, showing the yellow color of the typical $[Fe^{II}(BLPA)]$ complex. Upon exposure to O_2, **1** is converted to an intense blue species within a minute. This blue species exhibits two intense bands at 586 and 960 nm and EPR signals at g = 5.5 and 8.0 corresponding to the high-spin Fe(III) complex (S = 5/2, E/D = 0.11). This blue complex further reacts with O_2 to be converted to (μ-oxo)Fe^{III}_2 complex within a few hours. Interestingly, **1** affords intradiol cleavage (65%) and extradiol cleavage (20%) products after the oxygenation. It can be suggested that **1** undergoes two different oxygenation pathways. The one takes the substrate activation mechanism proposed for the intradiol cleavage products after the oxidation of the Fe^{II} to Fe^{III}. The other involves the direct attack of O_2 to Fe^{II} center, forming the Fe^{III}-superoxo intermediate which can give rise to the extradiol cleavage products. **1** is the first functional Fe(II) complex for extradiol-cleaving dioxygenases giving extradiol cleavage products.

Introduction

The catechol dioxygenases are non-heme iron enzymes that catalyze the oxidative cleavage of catechols and play a key role in detoxifying the aromatic pollutants in the environment.[1] They are found in soil bacteria with two different types: one is intradiol-cleaving enzyme utilizing Fe(III), and the other is extradiol-cleaving enzyme utilizing Fe(II) or Mn(II).[2-4] There has been a significant progress toward understanding the structure of active site and mechanism of the intradiol-cleaving enzymes. It was highlighted by the crystal structures of native protocatechuate 3,4-dioxygenase (3,4-PCD)[5,6] and 3,4-PCD-substrate complex[7] showing that the Fe(III) center of the active site has kept as a five-coordinate geometry. However, little is known for the extradiol-cleaving catechol dioxygenases. Spectroscopic studies[8-10] of catechol 2,3-dioxygenase (2,3-CTD) indicated the presence of square pyramidal high-spin Fe(II) center and EPR studies[11,12] of the 2,3-CTD-substrate·NO complex showed the binding site for NO (presumably O_2). Recently, the first crystal structure of the extradiol-cleaving dioxygenase, 2,3-dihydroxybiphenyl 1,2-dioxygenase (BphC), was reported that native enzyme has a Fe(II) center with a square pyramidal geometry with three endogenous protein ligands (two histidines and one glutamic acid) and two ligands from solvent (H_2O).[13,14] While the crystal structure of the enzyme-substrate complex shows Fe(III) instead of Fe(II) center, it has five-coordinate environment with an asymmetric didentate catecholate (DBCH), one glutamic acid, and two histidines.[14]

Model systems that mimic enzyme reactions are important mechanistic tools because the flexibility in ligand design allows a systematic investigation of the important factors affecting reactivity as well as reaction mechanism. In the previous biomimetic efforts, many scientists have focused on obtaining structurally characterized complexes capable of oxidative cleavage activity mimicking the intradiol dioxygenases.[15-24] Up to date, only two Fe(II) complexes, $[Fe^{II}(TLA)DBCH]BPh_4$ and $[Fe^{II}(Tp^{But Pri})DBCH]$ [25,26] have been reported as a structural mimic for extradiol-cleaving dioxygenase, where TLA is a tris(6-methylpyridylmethyl)amine, $Tp^{But Pri}$ is a hydrotris(3-*tert*-butyl-5-isopropyl-1-pyrazolyl)borate, and DBCH is 3,5-di-*tert*-butylcatecholate monoanion. However, neither complex showed any extradiol-cleaved products, instead obtained only intradiol-cleaved products for $[Fe^{II}(TLA)DBCH]BPh_4$ or no oxygenation product at all for $[Fe^{II}(Tp^{But Pri})DBCH]$.

In this paper, we report the synthesis, spectroscopic properties, and reactivity of $[Fe^{II}(BLPA)DBCH]BPh_4$ (**1**) which is the first Fe(II) complex giving the extradiol cleavage products. We also discuss the role of the metal center and the reaction mechanism in the oxygenation process of the extradiol-cleaving dioxygenases.

Materials and Methods

All reagents and solvents were purchased from commercial sources and used as received, unless noted otherwise. Acetonitrile was distilled from CaH_2 under nitrogen before use. $DBCH_2$ was purified by recrystallization from hexane. $DBCH_2$-4,6-d_2 was prepared by deuterium exchange in D_2O in the presence of a substoichiometric amount of base at 140 °C in a sealed tube for about 4 hours.[27] Microanalysis was performed by Korean Basic Science Research Institute, Seoul.

Synthesis of Bis((6-methyl-2-pyridyl)methyl)(2-pyridylmethyl)amine, BLPA. 1.28 g (10 mmol) 2-pyridylme-

thyl chloride was added slowly to 2.27 g (10 mmol) bis(6-methyl-2-pyridylmethyl)amine in 100 mL ethanol which was prepared according to the published procedure.[28] The reaction mixture was refluxed for 8 hours and concentrated under reduced pressure. The residue was dissolved in 30 mL CH_2Cl_2 and washed with water three times and then dried over anhydrous $MgSO_4$. The product was purified by silica gel column chromatography employing the eluent (ethyl-acetate : ethanol = 2 : 1) to afford a colorless solid (80% yield).

mp 84-85 °C, ^{1}H NMR ($CDCl_3$): δ 2.52 (s, Lu-CH_3), 3.85 (s, Lu-CH_2-), 3.88 (s, Py-CH_2-), 7.0 (d, Lu-β'), 7.1 (t, Py-β')′, 7.45 (d, Lu-β), 7.57 (t, Lu-γ), 7.65 (m, Py-β, γ), 8.5 (d, Py-α')′.

Synthesis of [Fe(BLPA)DBCH]BPh$_4$. [Fe(BLPA)DBCH]BPh_4 was synthesized by reacting 76.1 mg (0.60 mmol) $FeCl_2$ and 191.0 mg (0.60 mmol) BLPA in 15 mL ethanol under argon and adding 133.7 mg (0.60 mmol) $DBCH_2$ in 4 mL ethanol under argon followed by the slow addition of 1 equivalent triethylamine after 30 min. The resulting yellow solution was treated with 205.3 mg (0.60 mmol) $NaBPh_4$, causing the immediate precipitation of yellow powder, which was dried under vacuum (72% yield). Complex was purified by vapor diffusion of ether into an acetonitrile solution of crude product.

FAB^+-Mass m/z 595. Anal. Calcd. for [Fe(BLPA)DBCH]BPh_4, $C_{58}H_{62}BFeN_5O_2$: C, 75.08; H, 6.74; N, 7.55. Found: C, 75.28; H, 6.83; N, 7.51.

Characterization of Oxygenation Products. The four major and one minor organic products of the [Fe(BLPA)DBCH]$^+$ oxygenation reaction were identified by using GC, GC-Mass, HPLC, IR, and NMR spectroscopy. Spectroscopic data are as follows:

3,5-di-*tert*-butyl-5-(carboxymethyl)-2-furanone: IR (KBr) ν_{CO} 1755, 1723 cm^{-1}, $\nu_{C=C}$ 1644 cm^{-1}; ^{1}H NMR ($CDCl_3$): δ 0.96 (s, 9H), 1.21 (s, 9H), [2.74, 2.81, 2.91, 2.98 (AB q, J_{AB} = 14 Hz, 2H)], 6.93 (s, 1H), 9.70 (s); ^{13}C NMR ($CDCl_3$): δ 24.9 (q), 27.6 (q), 31.2 (s), 37.1 (t), 37.4 (s), 87.8 (s), 143.6 (s), 145.2 (d), 170.9 (s), 174.7 (s).

3,5-di-*tert*-butyl-1-oxacyclohepta-3,5-diene-2,7-dione: IR (KBr) ν_{CO} 1783, 1741 cm^{-1}, $\nu_{C=C}$ 1636, 1600 cm^{-1}; ^{1}H NMR ($CDCl_3$): δ 1.16 (s, 9H), 1.28 (s, 9H), 6.14 (d, J = 2 Hz, 1H), 6.45 (d, J = 2 Hz, 1H); ^{13}C NMR ($CDCl_3$): δ 28.4 (q), 28.9 (q), 36.2 (s), 36.5 (s), 115.5 (d), 123.9 (d), 148.0 (s), 160.0 (s), 162 (s).

3,5-di-*tert*-butyl-2-pyrone: IR (KBr) ν_{CO} 1710 cm^{-1}, $\nu_{C=C}$ 1635, 1560 cm^{-1}; ^{1}H NMR ($CDCl_3$): δ 1.20 (s, 9H), 1.32 (s, 9H), 7.04 (d, 1H), 7.14 (d, 1H); ^{13}C NMR ($CDCl_3$): δ 28.4 (q), 29.5 (q), 31.9 (s), 34.8 (s), 127.4 (s), 136.2 (s), 136.3 (s), 143.8 (d), 160.9 (s).

4,6-di-*tert*-butyl-2-pyrone: IR (KBr) ν_{CO} 1710 cm^{-1}, $\nu_{C=C}$ 1630, 1550 cm^{-1}; ^{1}H NMR ($CDCl_3$): δ 1.19 (s, 9H), 1.26 (s, 9H), 6.01 (d, 2H); ^{13}C NMR ($CDCl_3$): δ 28.1 (q), 29.0 (q), 35.5 (s), 36.2 (s), 98.7 (s), 107.2 (s), 163.4 (d), 167.7 (d), 171.4 (s).

3,5-di-*tert*-butyl-5-(formyl)-2-furanone: IR (KBr) ν_{CO} 1756, 1744, 1725 cm^{-1}; ^{1}H NMR ($CDCl_3$): δ 1.05 (s, 9H), 1.25 (s, 9H), 6.90 (s, 1H), 9.60 (s, 1H); ^{13}C NMR ($CDCl_3$): δ 24.8 (q), 28.1 (q), 32.2 (s), 38.5 (s), 94.5 (s), 141.3 (d), 146.1 (s), 170.5 (s), 197.3 (d).

Physical Methods. UV-visible spectra were obtained on a Hewlett-Packard 8453 biochemical analysis spectrophotometer. IR spectra were obtained by Bomem 102 FT-IR spectrometer. Standard organic product analyses were performed using a Hewlett-Packard 5890 Series II plus Gas Chromatograph equipped with a flame ionization detector or a reverse-phase isocractic HPLC (Orom Vintage 2000 high performance liquid chromatography; with a variable wavelength detector). Reaction mixtures were separated by using the C18 column. ^{1}H NMR spectra were obtained on a Varian VXR 300 and VXR 600 spectrometer. An inversion-recovery pulse sequence (180°-τ-90°-ACQ) was used to obtain non-selective proton longitudinal relaxation times (T_1) with carrier frequency set at several different positions to ensure the validity of the measurements.

Oxygenation Studies. Reactivity studies were performed in organic solvents in an oxygen atmosphere under ambient conditions. After the reaction was complete, as indicated by the loss of color, the solution was concentrated under reduced pressure. The organic products were extracted with ether, dried over anhydrous Na_2SO_4, and then concentrated. The remaining residue was dissolved in CH_2Cl_2 and acidified with HCl to pH 3 to decompose the (μ-oxo)Fe^{III}_2 complex. The furanonic acid was extracted with CH_2Cl_2, dried, and concentrated. The extracts were then subjected to GC or reverse-phase isocractic HPLC separation.

Results and Discussion

[Fe^{II}(BLPA)DBCH]BPh_4 (**1**) is a very air-sensitive yellow complex. The electronic spectrum of BLPA complex is dominated by an intense band at 386 nm (ε = 1700 M^{-1}cm^{-1}) in CH_3CN under argon (Figure 1). It has a slightly weaker intensities than that of [Fe^{II}(TLA)DBCH] complex (λ_{max} =

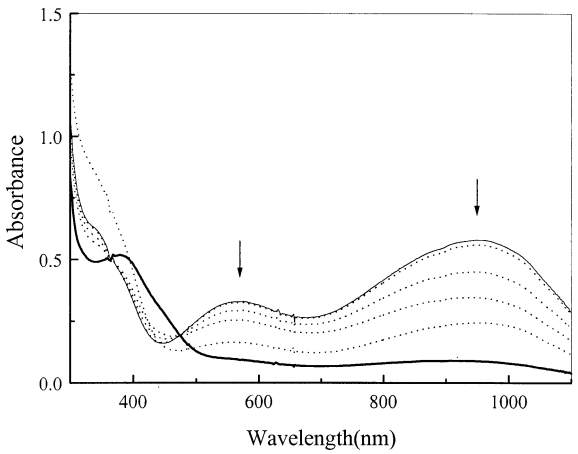

Figure 1. Electronic spectra showing the formation of [Fe^{III}(BLPA)DBC]$^+$ (solid line) upon exposure of [Fe^{II}(BLPA)DBCH]$^+$ (thick line) to O_2 in CH_3CN. The decay of catecholate-to-Fe(III) charge transfer bands was recorded as the oxygenation proceeded (dotted lines).

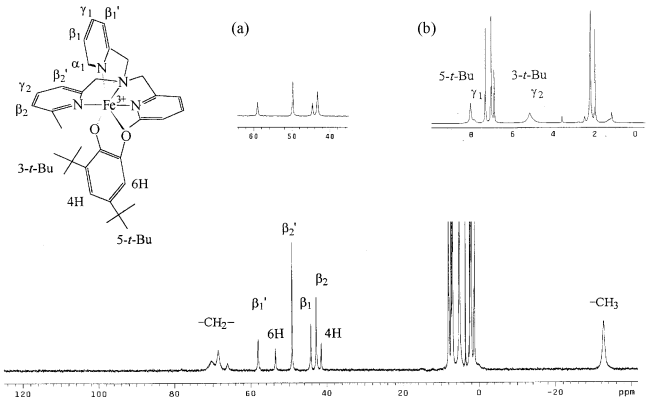

Figure 2. ^{1}H NMR spectrum of [Fe(BLPA)DBCH]BPh_4 in CD_3CN under argon with ambient conditions. The left inset (a) is a spectrum of [Fe^{II}(BLPA)DBCH-4,6-d_2]BPh_4. The right inset (b) is an expansion of diamagnetic region of the main spectrum. The two peaks at 7.3 and 6.9 ppm correspond to the protons of BPh_4 counter anion.

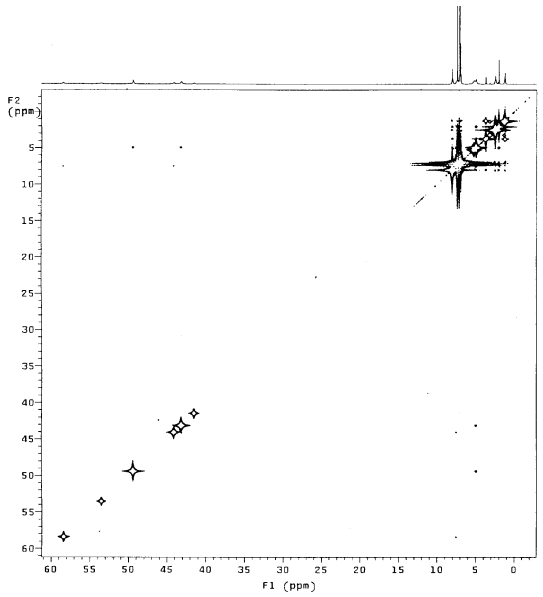

Figure 3. COSY spectrum of [Fe^{II}(BLPA)DBCH]BPh_4 in CD_3CN.

395 nm, ε = 2200 $M^{-1}cm^{-1}$).[25] This band can be assigned to the Fe^{II} to pyridine charge transfer band based on the extinction coefficient and the comparison with known [Fe^{II}(L)] complexes.[29] Upon exposure to O_2, [Fe^{II}(BLPA)DBCH]$^+$ is converted within a minute to intense blue species (λ_{max} = 586 and 960 nm). These bands are very similar to those of [Fe^{III}(BLPA)DBC]$^+$ complex (λ_{max} = 584 and 962 nm) which were assigned to catecholate-to-Fe^{III} charge transfer transitions.[30] We also observed the [Fe^{II}(BLPA)DBCH]$^+$ and [Fe^{III}(BLPA)DBC]$^+$ species during the mass spectrum run (FAB^+-Mass m/z: 595 and 594, respectively).

NMR Properties. The ^{1}H NMR spectrum of **1** displays relatively sharp well-resolved resonances due to the very favorable electronic relaxation time of the high-spin Fe(II) center (Figure 2).[31] The peaks were spread over a 150 ppm range. Most of protons can be assigned by comparison of integration, T_1 values, and COSY connectivity; the COSY information was particularly useful for identifying the ring protons of pendant picolyl and lutidyl ligands. The NMR spectrum of **1** is dominated by the beta protons of picolyl and lutidyl rings, which appear as relatively sharp features at 58, 43 and 49, 42 ppm with T_1 values of 9.5, 8.7 and 11.9, 7.2 ms, respectively. The picolyl alpha proton was quite broadened due to its proximity to the metal center and shifted further downfield at 140 ppm, whereas the lutidyl methyl protons appeared at -32 ppm with T_1 value of 1.3 ms. The gamma protons of picolyl and lutidyl rings resonate in the diamagnetic region at 7.7 ppm and 4.7 ppm, which were confirmed by COSY spectrum (Figure 3). Additional peaks arise from the methylene protons, which appear as a broad band at 68 ppm for picolyl and lutidyl with T_1 value of ~1.0 ms. The DBC 5-*t*-butyl and 3-*t*-butyl proton peaks are found at 7.7 and 4.7 ppm with T_1 values of 28.5 and 10.3 ms, respectively. The obscure peaks are confirmed by using the various delay times (d_1) of inversion-recovery (T_1) pulse in order to remove the diamagnetic signals. The DBC 6-H and 4-H protons of **1** exhibit shifts at 52 and 40 ppm with T_1 values of 6.4 and 6.7 ms, respectively, which were confirmed by the ^{1}H NMR spectrum of the selectively deuterated [Fe^{II}(BLPA)(DBCH-4,6-d_2)]BPh_4 complex (Figure 2).

EPR Properties. EPR spectroscopy is a very useful technique to study electronic state of the metal complex with half-integer electronic spin (Kramers system). It has been well established that one can also observe the EPR transitions even in the integer-spin systems (non-Kramers system).[32] Moreover, the intensities of these EPR transitions can be enhanced by changing the cavity in parallel mode which makes the microwave field parallel to the applied field ($B_1 \parallel B$). However we can observe the EPR transitions of the integer-spin systems both in parallel and perpendicular mode. EPR spectrum of **1** in CH_3CN at 4 K exhibits a broad signal at g = 9, which is a typical value of high-spin Fe(II) integer-spin system (S = 2), without any indication of semiquinone radical signals (Figure 4a).[31] Upon exposure to O_2, **1** is converted within a minute to intense blue species. This blue species exhibits EPR signals at g = 5.5 and 8.0 which are characteristic of the high-spin Fe(III) complex with almost axial symmetry (S = 5/2, E/D = 0.11), indicating that **1** is converted to the high-spin Fe^{III} complex (Figure 4b).[33] Furthermore, after the complete oxygenation, it shows a very weak EPR signal at g = 4.3 corresponding to the typical high-spin Fe^{III} species with rhombic symmetry (S = 5/2, E/D = 0.33).[33] But, most Fe(III) centers are EPR silent due to the antiferromagnetic coupling (S = 0) between high-spin Fe(III) centers (Figure 4c). This conversion resulted from the assembly of an (μ-oxo)Fe^{III}_2(BLPA)$_2$ complex with the furanonic acid bridging the two Fe(III) centers, whose NMR spectral property is very similar to that of the [Fe^{III}_2O(BLPA)$_2$(O_2CCH_3)] (ClO_4)$_3$ complex. Thus, **1** is converted to (μ-oxo)Fe^{III}_2 complex via [Fe^{III}(BLPA)DBC]$^+$ during the oxygenation.

Reactivity and Mechanism. After **1** is converted to [Fe^{III}(BLPA)DBC]$^+$ upon exposure to O_2, it further reacts with O_2 under pseudo-first order conditions and shows the

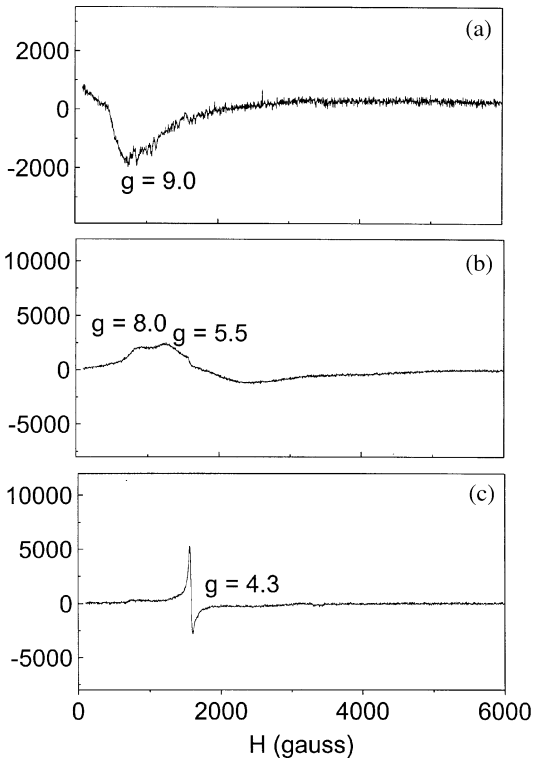

Figure 4. X-band EPR spectra: (a) $[Fe^{II}(BLPA)DBCH]BPh_4$ in CH_3CN under argon. (b) $[Fe^{II}(BLPA)DBCH]BPh_4$ in CH_3CN after the exposure to O_2 for 1 min. (c) $[Fe^{II}(BLPA)DBCH]BPh_4$ in CH_3CN after complete oxygenation. Spectra were obtained at 9.22 GHz with 100 kHz modulation at 4 K.

disappearance of catecholate-to-Fe(III) charge transfer bands (Figure 1). Interestingly, **1** reacts with O_2 within a few hours to afford intradiol and extradiol cleavage products resulting from C-C oxidative cleavage of the catechol ring. The intradiol cleavage products are 3,5-di-*tert*-butyl-1-oxacyclohepta-3,5-diene-2,7-dione (40%) and 3,5-di-*tert*-butyl-5-(carboxymethyl)-2-furanone (25%). The extradiol cleavage products are 3,5-di-*tert*-butyl-2-pyrone (8%), 4,6-di-tert-butyl-2-pyrone (12%), and 3,5-di-*tert*-butyl-5-(formyl)-2-furanone (trace amount). Our previous study showed that $[Fe^{III}(BLPA)DBC]^+$ gave intradiol (75%) and extradiol (15%) cleavage products,[29] and we further find that 1 gives more extradiol cleavage products. There have been only two model Fe(II) complexes for the extradiol-cleaving dioxygenases. The first one is $[Fe^{II}(TLA)DBCH]^+$ complex as a structural model of the extradiol-cleaving dioxygenase.[25] However, it gave only intradiol cleavage products (89%) after converting to Fe^{III} complex. Another model complex $[Fe^{II}(Tp^{But Pri})DBCH]$ did not give any oxidative cleavage product at all.[26] Thus, $[Fe^{II}(BLPA)DBCH]$ is the first complex to give the extradiol cleavage products among the Fe(II) model complexes.

There has been a proposed oxygenation mechanism for the extradiol-cleaving dioxygenases.[5] In this mechanism (Scheme 1), the first step appears to involve the activation of the substrate catecholate followed by the binding of O_2 to the Fe(II) center. Some electron transfer from metal to O_2 in the Fe(II)-O_2 species results in a superoxide-like moiety, which

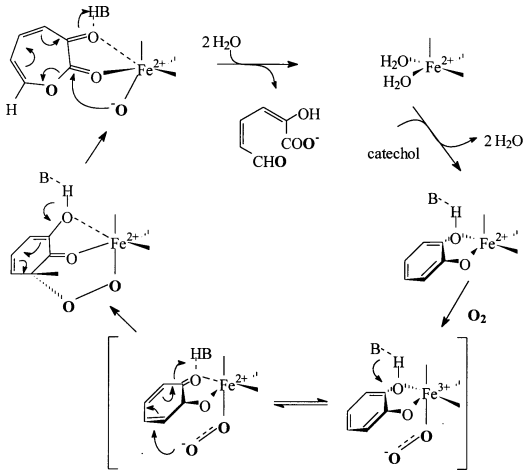

Scheme 1

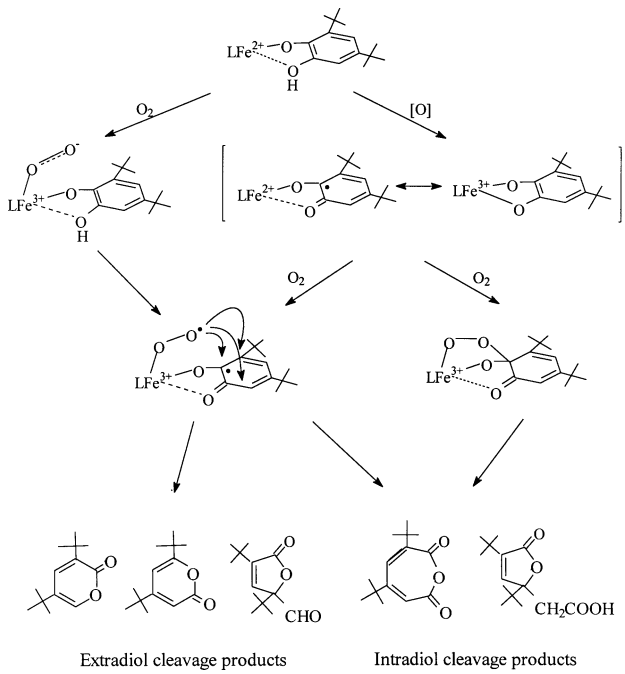

Scheme 2

gives the bound O_2 nucleophilic character. This bound O_2 attacks the carbon adjacent to the enediol unit in a Michael-type addition, to form a peroxy intermediate that decomposes by a Criegree-type rearrangement to the extradiol-cleavage products.

However, our experimental results show that the oxygenation process includes the oxidation of Fe(II) center to Fe(III) center and gives the intradiol cleavage products as major products and some extradiol cleavage products as minor products. Thus, we can propose that the substrate activation mechanism[34] is involved in the intradiol cleavage of catechol, in which O_2 attack on the coordinated catecholate is facilitated by the enhanced radical character of the substrate. A peroxide complex is proposed to form subsequently to O_2 binding and then decompose to the intradiol cleavage products.[18,35] In addtion, the extradiol cleavage products might be originated from the direct attack of O_2 to Fe(II)

center that makes the Fe(II)-O_2 species and converting to the peroxy intermediate during the oxygenation process.

Of course, we can not ignore the possibility that the extradiol cleavage products might come from the oxygenation of $[Fe^{III}(BLPA)DBC]^+$ as by-products. Consequently, we can suggest that **1** can undergo two different oxygenation pathways (Scheme 2). The first one takes the substrate activation mechanism after the oxidation of Fe(II) to Fe(III), and the second one might involve the direct attack of O_2 to the Fe(II) center, forming the Fe^{III}-superoxide intermediate which presumably gives the extradiol products.

The methyl substituent does interfere and control the oxygenation pathway similar to the effect of the hydrophobic pocket around the metal center in the real enzyme-substrate system. Thus, the geometry around the metal center can affect the specificity of the oxidative cleavage products. Therefore, we need to consider the steric effect as well as the electronic effect toward understanding the oxygenation process of catechol dioxygenases. Nevertheless, $[Fe^{II}(BLPA)DBCH]^+$ is the first functional Fe(II) complex for extradiol dioxygenases giving extradiol products. These results can provide the synthetic approach for Fe(II)-catecholate complexes preventing the oxidation of Fe(II) to Fe(III) and elucidate the oxygenation mechanism of extradiol-cleaving catechol dioxygenases.

Acknowledgment. The authors acknowledge the financial support of the Korea Research Foundation made in the program year of 1997.

References

1. Dekkar, M. In *Microbial Degradation of Organic Molecules*; Gibson, D. T., Ed.; New York, 1984.
2. Que, L., Jr. In *Iron Carriers and Iron Proteins*; Loehr, T. M., Ed.; VCH Publishers: New York, 1989; pp 467-524.
3. Lipscomb, J. D.; Orville, A. M. In *Metal ions in biological systems*; Sigel, H., Sigel, A., Eds.; New York, 1992; Vol. 28, pp 243-298.
4. Que, L., Jr.; Ho, R. Y. N. *Chem. Rev.* **1996**, *96*, 2607-2624.
5. Ohlendorf, D. H.; Lipscomb, J. D.; Weber, P. C. *Nature* **1988**, *336*, 403-405.
6. Ohlendorf, D. H.; Orville, A. M.; Lipscomb, J. D. *J. Mol. Biol.* **1994**, *244*, 586-608.
7. Orville, A. M.; Lipscomb, J. D.; Ohlendorf, D. H. *Biochemistry* **1997**, *36*, 10053-10066.
8. Mabrouk, P. A.; Orville, A. M.; Lipscomb, J. D.; Solomon, E. I. *J. Am. Chem. Soc.* **1991**, *113*, 4053-4061.
9. Bertini, I.; Briganti, F.; Mangani, S.; Nolting, H. F.; Scozzafava, A. *Biochemistry* **1994**, *33*, 10777-10784.
10. Shu, L.; Chiou, Y-M.; Orville, A. M.; Lipscomb, J. D.; Que, L., Jr. *Biochemistry* **1995**, *34*, 6649-6659.
11. Arciero, D. M.; Orville, A. M.; Lipscomb, J. D. *J. Biol. Chem.* **1985**, *260*, 14035-14044.
12. Arciero, D. M.; Lipscomb, J. D. *J. Biol. Chem.* **1986**, *261*, 2170-2178.
13. Han, S.; Eltis, L. D.; Timmis, K. N.; Muchmore, S. W.; Bolin, J. T. *Science* **1995**, *270*, 976-980.
14. Senda, T.; Sugiyama, K.; Narita, H.; Yamamoto, T.; Kimbara, K.; Fukuda, M.; Sato, M.; Yano, K.; Mitsui, Y. *J. Mol. Biol.* **1996**, *255*, 735-752.
15. Funabiki, T.; Mizoguchi, A.; Sugimoto, T.; Tada, S.; Tsuji, M.; Yoshioka, T.; Sakamoto, H.; Takano, M.; Yoshida, S. *J. Am. Chem. Soc.* **1986**, *108*, 2921-2932.
16. Que, L. Jr.; Kolanczyk, R. C.; White, L. S. *J. Am. Chem. Soc.* **1987**, *109*, 5373-5380.
17. Cox, D. D.; Benkovic, S. J.; Bloom, L. M.; Bradley, F. C.; Nelson, M. J.; Que, L., Jr.; Wallick, D. E. *J. Am. Chem. Soc.* **1988**, *110*, 2026-2032.
18. Cox, D. D.; Que, L., Jr. *J. Am. Chem. Soc.* **1988**, *110*, 8085-8092.
19. Jang, H. G.; Cox, D. D.; Que, L., Jr. *J. Am. Chem. Soc.* **1991**, *113*, 9200-9204.
20. Dei, A.; Gatteschi, D.; Pardi, L. *Inorg. Chem.* **1993**, *32*, 1389-1395.
21. Koch, W. O.; Krüger, H.-J. *Angew. Chem. Int. Ed. Engl.* **1995**, *34*, 2671-2674.
22. Ito, M.; Que, L., Jr. *Angew. Chem. Int. Ed. Engl.* **1997**, *36*, 1342-1344.
23. Duda, M.; Pascaly, M.; Krebs, M. *J. Chem. Soc., Chem. Commun.* **1997**, 835-836.
24. Viswanathan, R.; Palaniandavar, M.; Balasubramanian, T.; Muthiah, T. P. *Inorg. Chem.* **1998**, *37*, 2943-2951.
25. Chiou, Y-M.; Que, L. Jr. *Inorg. Chem.* **1995**, *34*, 3578-3579.
26. Ogihara, T.; Hikichi, S.; Akita, M.; Moro-oka, Y. *Inorg. Chem.* **1998**, *37*, 2614-2615.
27. Pyrz, J. W.; Roe, A. L.; Stern, L. J.; Que, L., Jr. *J. Am. Chem. Soc.* **1985**, *107*, 614-620.
28. de Mota, M. M.; Rodgers, J.; Nelson, S. N. *J. Chem. Soc.*(A) **1969**, 2036-2044.
29. Zang, Y.; Elgren, T. E.; Dong, Y.; Que, L., Jr. *J. Am. Chem. Soc.* **1993**, *115*, 811-813.
30. Lim, J. H.; Lee, H.-J.; Lee, K.-B.; Jang, H. G. *Bull. Korean Chem. Soc.* **1997**, *18*, 1166-1172.
31. Bertini, I.; Luchinat, C. *NMR of Paramagnetic Molecules in Biological Systems*; The Benjamin/Cummings Publishing Company Inc.: California, 1986.
32. Hendrich, M. P.; Debrunner, P. G. *Biophys. J.* **1989**, *56*, 489-506.
33. Wertz, J. E.; Bolton, J. R. *Electron Spin Resonance; Elementary theory and Practical Applications*; Chapman and Hall: New York, London, 1986.
34. Que, L. Jr.; Lipscomb, J. D.; Münck, E.; Wood, J. M. *Biochim. Biophys. Acta* **1977**, *485*, 60-74.
35. Barbaro, P.; Bianchini, C.; Mealli, C.; Meli, A. *J. Am. Chem. Soc.* **1991**, *113*, 3181-3183.